Int J Thermophys (2010) 31:1428–1437
DOI 10.1007/s10765-010-0802-0

Dielectric-Constant Gas-Thermometry Scale from 2.5 K to 36 K Applying ^{3}He, ^{4}He, and Neon in Different Temperature Ranges

C. Gaiser · B. Fellmuth · N. Haft

Received: 11 March 2010 / Accepted: 19 July 2010 / Published online: 14 August 2010

Abstract New dielectric-constant gas-thermometry (DCGT) measurements were performed at PTB in the temperature range from 23 K to 36 K. For the first time, besides helium, neon was also used as a measuring gas. The measurements with helium and neon yielded thermodynamic temperature data in the range between 27 K and 36 K. A combination of these data, with former measurements in the range between 2.5 K and 26 K made using ^{3}He and ^{4}He, lead to a temperature scale which coincides with the ITS-90 within a few tenths of a millikelvin even at highest temperatures. The discussion of the uncertainty budget for neon follows the procedures already proved for helium. Furthermore, a comparison between new highly accurate *ab initio* calculations for the second and third density virial coefficients of helium, and the extended DCGT results are given. For the third virial coefficient of helium, the presented data allow the first experimental check of the new *ab initio* calculation for the range above 24 K.

Keywords Helium · Low temperatures · Neon · Primary thermometry · Virial coefficients

1 Introduction

Dielectric-constant gas thermometry (DCGT), in over 25 years, has been a well-established method for primary thermometry at PTB. The two generations of DCGT led to results for the thermodynamic temperature between 2.5 K and 27 K [1–3] with a standard uncertainty of a few tenths of a millikelvin in the whole range. Whereas the main goal of the first generation was to check the existing thermodynamic

C. Gaiser (✉) · B. Fellmuth · N. Haft
Physikalisch-Technische Bundesanstalt, Abbestr. 2-12, 10587 Berlin, Germany
e-mail: christof.gaiser@ptb.de

temperature data with an independent method, the second generation was used for an efficiency test to demonstrate that DCGT is capable of determining the Boltzmann constant at the triple point of water (TPW) [4]. Compared with [2,5], the benefit of the extension of the DCGT temperature scale to 36 K presented in this article is threefold. Primarily, the existing thermodynamic temperature data above 27 K are inconsistent and, therefore, new measurements are strongly recommended to allow a clarification [6]. Secondly, the determination of the dipole polarizability of neon [7] will be needed for consistency checks at the TPW (use of different gases to verify the estimated equipment parameters). Thirdly, in addition to the extended comparison of experimental values for the second virial coefficient of helium with theoretical values up to 36 K, for the first time a comparison with two different theories is possible for the third virial coefficient. This is of special interest because, over the last decade, large progress was achieved in theory concerning two- and three-particle interactions between helium atoms [8–10]. This article is organized as follows: Sect. 2 gives a brief review of the DCGT method, the data evaluation, and the experimental setup; Sects. 3.1 and 3.2 state the uncertainty of the measurements made with helium and neon, respectively, in Sect. 3.3 all the DCGT measurements performed at PTB using ^{3}He, ^{4}He, and neon are summarized and discussed; and Sect. 4 provides the conclusions.

2 Measurements

2.1 Theory

2.1.1 DCGT Principle

The basic idea of DCGT [11], more extensively discussed in [1,2,12], is to replace the density in the equation of state of a gas with the dielectric constant, ε, and to measure it by incorporating a capacitor in the gas bulb. The dielectric constant of an ideal gas is given by the relation $\varepsilon = \varepsilon_0 + \alpha_0 N/V$, where ε_0 is the exactly known electric constant, α_0 is the static electric dipole polarizability of the particles, and N/V is the number density, i.e., the equation of state of an ideal gas can be written in the form $p = kT(\varepsilon - \varepsilon_0)/\alpha_0$. Absolute DCGT requires a knowledge of α_0 with the necessary accuracy. A sufficiently accurate theoretical calculation of α_0 is only possible for helium, where recent progress has decreased the uncertainty of the *ab initio* value well below one part in 10^6 [13,14]. The molar polarizability, A_ε, is defined as $A_\varepsilon = N_A\alpha_0/(3\varepsilon_0)$. For a real gas, the interaction between the particles has to be considered by combining the virial expansions of the equation of state and the Clausius–Mossotti equation. Neglecting higher-order terms and the third dielectric virial coefficient, this yields

$$p \approx \frac{\chi}{\frac{3A_\varepsilon}{RT} + \kappa_{\mathrm{eff}}}\left[1 + \frac{B^*(T)}{3A_\varepsilon}\chi + \frac{C(T)}{(3A_\varepsilon)^2}\chi^2 + \cdots\right], \tag{1}$$

where $\chi = \varepsilon/\varepsilon_0 - 1$ is the dielectric susceptibility, $B^*(T) = B(T) - b(T)$, $B(T)$ and $C(T)$ are the second and third density virial coefficients taking into account

the pair and triplet interactions, respectively, $b(T)$ is the second dielectric virial coefficient, and κ_{eff} is the effective compressibility of the capacitor used to measure the susceptibility χ. To determine $3A_\varepsilon/(RT)$, isotherms have to be measured, i.e., the relative change in capacitance $(C_{\text{M}}(p) - C_{\text{M}}(0))/C_{\text{M}}(0) = \chi + (\varepsilon/\varepsilon_0)\kappa_{\text{eff}}\, p$ of the gas-filled measuring capacitor is determined as a function of the pressure p of the gas. The capacitance $C_{\text{M}}(p)$ of the capacitor is measured with the space between its electrodes filled with the gas at various pressures and with the space evacuated so that $p = 0\,\text{Pa}$. A polynomial fit to the resulting p versus $(C_{\text{M}}(p) - C_{\text{M}}(0))/C_{\text{M}}(0))$ data points, together with a knowledge of the pressure dependence of the dimensions of the capacitor (effective compressibility κ_{eff}), yields $3A_\varepsilon/(RT)$. Since the susceptibilities of gases are very small, they cannot be determined *via* absolute capacitance measurements. Even the required measurement of the relative capacitance changes to an uncertainty of a few parts in 10^9 places extreme demands on the parameters of the audio-frequency capacitance bridge.

2.1.2 Data Evaluation Via Multi-isotherm Fits

The procedure used for the multi-isotherm fitting was extensively discussed in [1,12]. Only a short summary will be given here. In principle, the complete information from the experiment, temperature as well as the virial coefficients, can be extracted from an isotherm by a single-isotherm fit according to Eq. 1. Facing the fact that a usual isotherm consists of seven data points and the fitting order is three, the amount of data is only a factor of two larger than the degrees of freedom. Even though this is enough for most purposes, it can be shown that an uncertainty reduction by a factor of two is possible if all isotherms are fitted together. Such a so-called multi-isotherm fit is only achievable if all data points for different temperatures can be transferred to one virtual isotherm. Temperature expansions for the virial coefficients are the means to affect such a transfer. In the past, several different expansions have been discussed, but only the most recent ones, presented in [5], have a complete theoretical basis [15,16]:

$$B(T) = b_1 + b_2 T^{-1.5} + b_3 T^{-1} + b_4 T, \tag{2}$$

$$C(T) = c_1 + c_2 T^{-3} + c_3 T^{-2} + c_4 T^{-1.5}. \tag{3}$$

These expansions are exclusively used here for the data evaluation *via* multi-isotherm fits.

2.2 Experiment

2.2.1 Changes Made to the Former DCGT Setup

The experimental setup of the present DCGT has been described in detail in [2]. Only slight changes concerning the thermometric setup have been performed. Particularly, two different sensors with optimized sensitivities were used for temperature control above and below 20 K. Therefore, even at the highest temperature, the temperature instability of the experimental cell was on the order of 100 μK. Besides

the precision rhodium–iron-resistance thermometers, which carry the PTB copy of the gas-thermometer scale NPL-75 [17] as one basis of the International Temperature Scale of 1990 (ITS-90) [18], two standard platinum-resistance thermometers calibrated according to the ITS-90 at PTB have been added to the experimental cell.

2.2.2 Data

At temperatures of 23 K, 24.5 K, 27 K, 28 K, and in steps of 2 K up to 36 K, isotherms were obtained with ^{4}He as the measuring gas. For each isotherm, measurements at seven pressures were usually performed during 1 day. This leads to a dataset of 230 triplets of pressure, susceptibility, and temperature. Neon isotherms were taken at 23 K, 24 K, 24.5 K, 25 K, 26 K, and further at the same higher temperatures as with helium. The maximum pressure was kept below half of the condensation pressure of Ne. Measurements on different days were made at the same temperature and different pressures to increase the number of triplets on merged isotherms to a maximum of 14 triplets. This led to a dataset of 131 triplets for neon.

3 Results

3.1 Uncertainty Budgets for the Results Obtained with Helium

Uncertainty budgets for thermodynamic temperature values obtained with helium applying DCGT from 2.4 K to 26 K have been published in [2,12]. Besides minor changes in estimating some uncertainty components, the most important change in the new budgets around and above 26 K occurred due to the fact that the components resulting from testing the use of different temperature expansions for the virial coefficients in a multi-isotherm fit became smaller. The spread of the results is decreased because of the increase in the number of input data. Therefore, the overall standard uncertainty at 26 K is now 0.32 mK (instead of 0.40 mK in [2]) and 0.54 mK at 36 K. The uncertainty budgets for the virial coefficients up to 26 K [5,12] are not affected by the mentioned changes. An evaluation of the different components led to an uncertainty at 36 K of 0.02 $\mathrm{cm}^3 \cdot \mathrm{mol}^{-1}$ for B^* and of 14.3 $\mathrm{cm}^6 \cdot \mathrm{mol}^{-2}$ for C.

3.2 Uncertainty Budgets for the Results Obtained with Neon

Following exactly the same formalism as used for helium, the uncertainty budgets for neon have been established. The type A components have been estimated *via* Monte–Carlo simulations implemented in the multi-isotherm fit routine. The correction of neon layers on the capacitor electrodes has been performed as for helium [12], and the considered number of layers has been checked against literature data [19] showing very good agreement. A drastic increase of the estimates with decreasing temperature is a general trend. This is due to the drastic decrease of the vapor pressure below 27 K and, therefore, the very small measuring signal at the capacitance bridge.

Measurements below 23 K with neon could not be reasonably conducted. Similar arguments hold for the pressure measurement.

The uncertainty of the polarizability of neon has to be included as an important type B component for DCGT measurements. (This component is negligible for helium, see Sect. 2.1.1.) The molar polarizability value for neon of $A_\varepsilon = 9.94727(11) \times 10^{-07}\ \mathrm{m}^3 \cdot \mathrm{mol}^{-1}$ used in this work, is the weighted mean of results from seven pairwise combined helium and neon isotherms, described in more detail in [7]. Another important component is the possible influence of impurities on the polarizability. It was stated by the manufacturer that the ultra-pure 99.9993 % neon used in the experiments has a content of helium of at most 3 ppm. But for hydrogen, the manufacturer did not state the content. Measurements using an ultra-precise quadrupole mass spectrometer revealed a content of 5 ppm of helium and 4 ppm of hydrogen. The influences of these two elements, which are the only non-condensed impurities in the treated temperature range, may partly compensate themselves (helium has a polarizability about a factor of two smaller than that of neon, but that of hydrogen is larger by nearly the same factor). Nevertheless, the individual estimates for the influence were summed in quadrature leading to the estimate considered in the uncertainty budget, see Table 1. The other type B components have been treated the same as for helium. It is worth mentioning that for neon, the impact of the uncertainty of κ_{eff} is approximately one half that of helium due to the larger polarizability. A complete uncertainty budget for the thermodynamic temperature measured with neon is given in Table 1.

Table 1 Uncertainty budget for DCGT measurements using neon as measuring gas

Component	23 K	26 K	30 K	36 K
Monte–Carlo simulations (type A components)[a]				
Susceptibility	0.67	0.38	0.33	0.35
Pressure repeatability	0.21	0.10	0.08	0.07
Temperature instability	0.10	0.04	0.08	0.11
Ne layers	0.79	0.49	0.21	0.30
Effective compressibility	0.05	0.06	0.08	0.11
Type B estimates[b]				
Pressure (A_{eff})	0.12	0.13	0.15	0.18
Impurity layers	0.03	0.04	0.04	0.05
Aerostatic head	0.15	0.16	0.18	0.20
Impurities in the gas	0.10	0.11	0.13	0.16
Polarizability (A_ε)	0.24	0.28	0.32	0.38
Combined standard uncertainty	1.10	0.73	0.59	0.70

Since especially below 27 K the uncertainty changes drastically, four temperature values resulting from a multi-isotherm fit to the DCGT data are shown. The estimates are given in mK

[a] These uncertainty estimates are based on Monte–Carlo simulations performed with one hundred data sets randomized with the standard deviation of the specific quantity

[b] These uncertainty estimates are based on calibrations and comparisons of pressure balances for determining the effective area A_{eff}, on literature data for the typical thickness of impurity layers on the capacitor plates, and analysis data (mass spectroscopy) for impurity concentrations in the measuring gas

3.3 Thermodynamic Temperature Results

The large amount of thermodynamic temperature data taken with DCGT allows for a scale between 2.5 K and 36 K. Figure 1 shows different sets of differences $T_{\mathrm{DCGT}} - T_{90}$ (T_{DCGT} and T_{90} are DCGT and ITS-90 temperature values, respectively) starting with the first generation of DCGT at PTB (DCGT1) [1] between 4.2 K and 27 K. In the same range, the second generation (DCGT2) yielded an uncertainty of about a factor of two smaller than that for DCGT1. At the low temperature end, the ^{4}He data already published in [5] is expanded using ^{3}He measurements published in [3]. The data are further complemented with the new data up to 36 K described in Sect. 2.2.2. Above 26 K, the differences $T_{\mathrm{DCGT}} - T_{90}$ for ^{4}He are based on a complete multi-isotherm fit to all data between 3.7 K and 36 K using the temperature expansions for the virial coefficients given by Eqs. 2 and 3. The first results obtained with neon are also

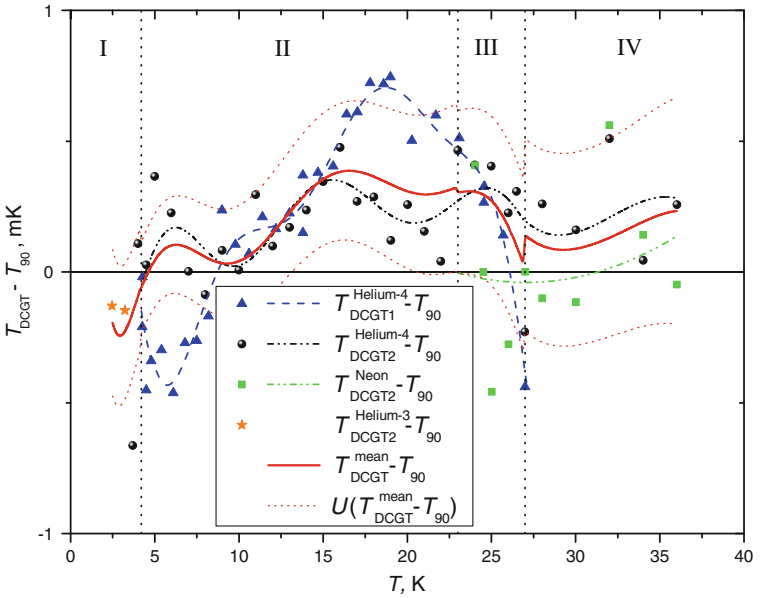

Fig. 1 Deviations of the DCGT temperature values, T_{DCGT}, measured with two different setups (DCGT1 [1] and DCGT2 [2]) from the ITS-90 [18] temperature values, T_{90}. The ^{4}He datasets of DCGT1 [1] (*blue triangles*) and DCGT2 (*black dots*) have been evaluated *via* multi-isotherm fits (for details, see text). The results of two measurements made with ^{3}He [3] are plotted as *orange asterisks*. The results obtained with DCGT2 using neon as measuring gas are also shown, as *green squares*. The smooth differences $\Delta T = T_{\mathrm{DCGT}} - T_{90}$ for the DCGT1 dataset (*dashed blue line*) and the DCGT2 dataset (*dashed-dotted black line*) have been approximated using polynomial fits of ninth order to the experimental differences. For neon a fit of second order (*dashed-dotted green line*) was sufficient. In addition, the difference $T^{\mathrm{mean}}_{\mathrm{DCGT}} - T_{90}$ (*red line*), resulting from a weighted mean of all shown DCGT data, and the related confidence intervals $U(T^{\mathrm{mean}}_{\mathrm{DCGT}} - T_{90})$ corresponding to the standard uncertainty $u(T^{\mathrm{mean}}_{\mathrm{DCGT}} - T_{90})$ ($k = 1$, *dotted red lines*) are shown. The plot is divided in four regions, in which different data are used: (I) (2.5 K to 4.2 K) only DCGT2 data obtained with ^{3}He and ^{4}He, (II) (4.2 K to 23 K) DCGT1 and DCGT2 with ^{4}He, (III) (23 K to 27 K) DCGT1 and DCGT2 with ^{4}He, DCGT2 with neon, and (IV) (27 K to 36 K) DCGT2 with ^{4}He and neon. This is the reason why at the crossover from one region to the other, the mean curve is not smooth. (color figure online)

Table 2 Deviation of the weighted mean of the DCGT2 data $T_{\mathrm{DCGT}}^{\mathrm{mean}}$, measured with ^{4}He and neon, from T_{90} values together with the related uncertainty estimates

T (K)	$T_{\mathrm{DCGT}}^{\mathrm{mean}} - T_{90}$ (mK)	$u(T_{\mathrm{DCGT}}^{\mathrm{mean}} - T_{90})$ (mK)	$B^*(T)$ (cm$^3 \cdot$ mol^{-1})	$C(T)$ (cm$^6 \cdot$ mol^{-2})
27.0	0.14	0.34	2.43	264.5
28.5	0.09	0.34	3.19	259.9
30.0	0.09	0.34	3.87	256.1
31.5	0.12	0.35	4.48	252.8
33.0	0.16	0.36	5.03	250.0
34.5	0.21	0.38	5.53	247.6
36.0	0.23	0.41	5.99	245.6

In addition, the DCGT2 values for $B^*(T)$ and $C(T)$ of ^{4}He, calculated with the coefficients given in Table 3 employing Eqs. 2 and 3, are listed

shown. The smooth curves drawn in Fig. 1 resulted from fits to the sets of differences $T_{\mathrm{DCGT}} - T_{90}$. The two sets obtained with DCGT1 and DCGT2, respectively, using ^{4}He were each fitted with a polynomial of ninth order. For neon, a polynomial of second order was sufficient. The smooth polynomials have been used to deduce weighted means with the weights related to the uncertainties (for DCGT1, see [1]; for DCGT2, see [2], Sects. 3.1 and 3.2). The weighted means of the smoothed differences and their uncertainties, including the uncertainty of the realization of the ITS-90, are also shown in Fig. 1 and listed in Table 2 above 26 K. It is visible that the deviations of the mean DCGT temperature values from the ITS-90 are on the level of at most ±0.3 mK over the whole temperature range. It should be pointed out that the measurements with neon are not completely independent of those with helium, because the polarizability value has been determined *via* a special partial link between neon and helium data from 26 K to 36 K [7]. Therefore, the agreement between the temperature results is mandatory. But the neon measurements yield additional experimental information, which allows checking if there would be a continuously changing deviation between the thermodynamic temperature and the ITS-90. Such a tendency does obviously not exist. In summary, the ITS-90 is proven to be in very good agreement with thermodynamic temperature values obtained with DCGT between 2.5 K and 36 K.

3.4 Results for the Second and Third Virial Coefficients of ^{4}He

Recently, results for the second and third virial coefficients $B^*(T)$ and $C(T)$ of ^{4}He and a comparison with *ab initio* values in the range between 3.7 K and 26 K have been published [5]. The main focus of this section lies, therefore, on the extension to 36 K. Figure 2 shows the deviation of the latest results for the second virial coefficient $B^*(T)$ determined *via* DCGT from a combined *ab initio* theory; $B^*(T) = B(T) - b(T)$ is plotted ($B(T)$ from [8] and $b(T)$ from [20]). The DCGT data have been evaluated *via* the multi-isotherm fit using Eqs. 2 and 3 from 3.7 K to 36 K that led to the coefficients listed in Table 3. (It should be mentioned that the results for $B^*(T)$ presented here

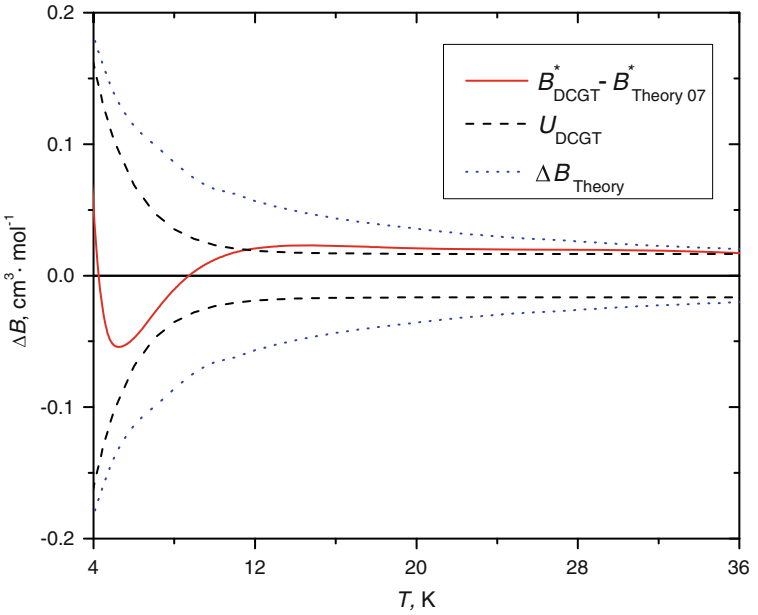

Fig. 2 Comparison of *ab initio* theory data $B^*_{\mathrm{Theory07}} = B_{\mathrm{Theory}} - b_{\mathrm{Theory}}$ from [8,20] and DCGT results for the second virial coefficient B^*_{DCGT} of ^{4}He determined *via* a multi-isotherm fit to the data between 3.7 K and 36 K ($\Delta B = B^*_{\mathrm{DCGT}} - B^*_{\mathrm{Theory07}}$, *red line*). The values for B^*_{DCGT} can be calculated using Eq. 2 and the coefficients listed in Table 3. The confidence intervals U_{DCGT} corresponding to the standard uncertainty u_{DCGT} ($k = 1$) for B^*_{DCGT} are also shown (*black dashed lines*). (u_{DCGT} has been determined *via* Monte–Carlo simulations, see Sect. 3.2 and [5]). In addition, for comparison purposes and to get an indication of the spread of the theoretical results, the difference $\Delta B_{\mathrm{Theory}}$ between the latest *ab initio* theories [8,9] is plotted (*blue dotted line*). (color figure online)

Table 3 Fitting coefficients obtained for ^{4}He by a multi-isotherm fit in the range from 3.7 K to 36 K using the expansions in Eq. 2 for $B^*(T)$ and in Eq. 3 for $C(T)$

$B^*(T)(\mathrm{cm^3 \cdot mol^{-1}})$ (Eq. 2)	DCGT2 (3.7 K to 36 K)	$C(T)(\mathrm{cm^6 \cdot mol^{-2}})$ (Eq. 3)	DCGT2 (3.7 K to 36 K)
b_1 ($\mathrm{cm^3 \cdot mol^{-1}}$)	18.6236	c_1 ($\mathrm{cm^6 \cdot mol^{-2}}$)	230.044
b_2 ($\mathrm{K^{1.5} \cdot cm^3 \cdot mol^{-1}}$)	0.28125	c_2 ($\mathrm{K^3 \cdot cm^6 \cdot mol^{-2}}$)	−173080.3
b_3 ($\mathrm{K \cdot cm^3 \cdot mol^{-1}}$)	−414.349	c_3 ($\mathrm{K^2 \cdot cm^6 \cdot mol^{-2}}$)	73952.44
b_4 ($\mathrm{K^{-1} \cdot cm^3 \cdot mol^{-1}}$)	−0.03135	c_4 ($\mathrm{K^{1.5} \cdot cm^6 \cdot mol^{-2}}$)	−8169.370

agree with the recently published values [5] up to 26 K, well within their uncertainty estimates). In addition, the uncertainty estimates evaluated *via* Monte–Carlo simulation (see Sect. 3.2) are given. For the uncertainty of the theory, no clear statement is contained in [8]. To give the reader an impression of the differences still existing in the latest *ab initio* calculations for $B(T)$, the differences between the values published in [8,9] are also plotted. It is visible that for $B(T)$ in this temperature range, the reliability of experimental and theoretical results is on a par, and theory and experiment are in very good agreement.

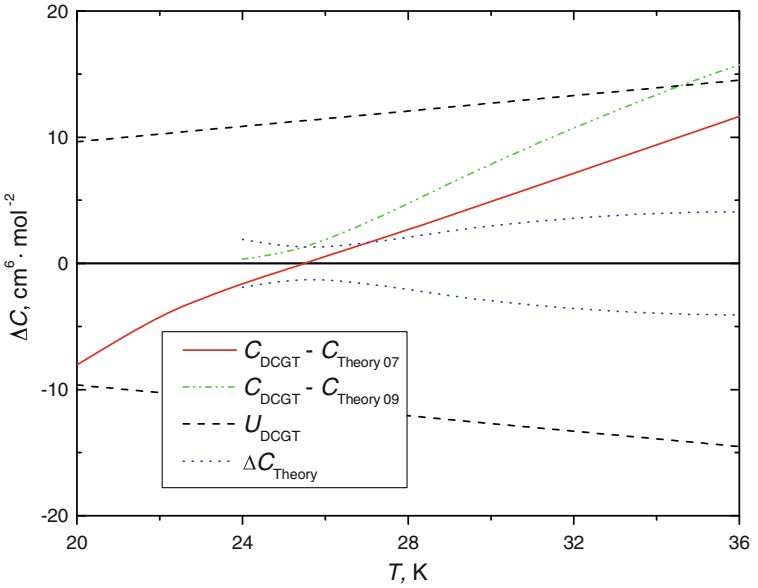

Fig. 3 Comparison of two different *ab initio* calculations for C, C_{Theory07} [8] and C_{Theory09} [10], with the experimental data for the third virial coefficient C_{DCGT} of ^{4}He determined *via* a multi-isotherm fit to the DCGT data between 3.7 K and 36 K ($\Delta C = C_{\mathrm{DCGT}} - C_{\mathrm{TheoryXX}}$, *red full* and *dashed-dotted green line*). The values for C_{DCGT} can be calculated using Eq. 3 and the coefficients listed in Table 3. The confidence intervals U_{DCGT} corresponding to the standard uncertainty $u_{\mathrm{DCGT}}(k = 1)$ for C_{DCGT} are also shown (*black dashed lines*). (u_{DCGT} has been determined *via* Monte–Carlo simulations, see Sect. 3.2 and [5].) In addition, for comparison purposes and to get an indication of the spread of the theoretical results, the difference $\Delta C_{\mathrm{Theory}}$ between C_{Theory07} [8] and C_{Theory09} [10] is plotted (*blue dotted line*). (color figure online)

For the three-particle interactions expressed in the third virial coefficient $C(T)$, the data are shown in Fig. 3 in the temperature range accessible by the *ab initio* theories, whereas the experimental results given in Table 3 are valid for the complete range between 3.7 K and 36 K. (Again it should be mentioned that the results for $C(T)$ presented here agree with the recently published values [5] up to 26 K, well within their uncertainty estimates.) Two lines in Fig. 3 show the deviation of the DCGT results from the *ab initio* values published in [8] and [10], respectively. The *ab initio* calculations are completely different in so far as in [8], the two-body potential was used to reconstruct a quasi-three-body potential. Also, quantum corrections were introduced. In [10], the first real three-body potential was calculated using a path-integral method. The main advantage of this theory is that the repulsive part of the three-particle interaction is treated, which is not the case in [8], i.e., especially at intermediate and higher temperatures, the newest theory is more reliable. But the theory in [10] is fully based on Boltzmann statistics, which might lead, as a disadvantage, to wrong results in the low-temperature range, where quantum effects become relevant. Concerning the uncertainty of the theories, the situation is similar to that for $B(T)$. In addition to the experimental uncertainty determined *via* Monte–Carlo simulations, the difference between both theories is plotted. The difference between theory and experiment

is within the uncertainty of the experiment. Nevertheless, the increasing deviation with temperature is remarkable. Thus, future experiments at higher temperatures, e.g., around the triple point of argon, are desirable to see if this tendency is only due to lack of high-temperature data or if there are other reasons.

4 Conclusions

The combination of data from 2.5 K to 36 K, obtained with two different DCGT setups and three different measuring gases, led to a thermodynamic temperature scale being in accordance with the ITS-90 within a few tenths of a millikelvin. Very recently, doubts arose concerning the validity of the ITS-90 in the range between the triple points of neon (25 K) and argon (84 K) [6]. Thus, the presented DCGT results underpin the necessity of additional thermodynamic temperature measurements in this temperature range.

Concerning the second virial coefficient of ^{4}He, very good agreement between the experimental data and the results of theoretical *ab initio* calculations has been found, being an additional efficiency proof of DCGT. For the third virial coefficient, the agreement was within the uncertainty of the experiment, but an increasing deviation between theory and experiment was observed, which has to be investigated in the future at higher temperatures.

References

1. H. Luther, K. Grohmann, B. Fellmuth, Metrologia **33**, 341 (1996)
2. C. Gaiser, B. Fellmuth, N. Haft, Int. J. Thermophys. **29**, 18 (2008)
3. C. Gaiser, B. Fellmuth, Europhys. Lett. **83**, 15001 (2008)
4. B. Fellmuth, Ch. Gaiser, J. Fischer, Meas. Sci. Technol. **17** (2006)
5. B. Gaiser Fellmuth, Metrologia **46**, 525 (2009)
6. J. Fischer, M. DePodesta, K.D. Hill, M.R. Moldover, L. Pitre, P.P.M. Steur, D.R. White, O. Tamura, I. Yang, Working Group 4 Report to the Consultative Committee for Thermometry, BIPM document CCT/08-13/rev (2008)
7. C. Gaiser, B. Fellmuth, EPL **90**, 63002 (2010)
8. E. Bich, R. Hellmann, E. Vogel, Mol. Phys. **105**, 3035 (2007)
9. J.B. Mehl, C.R. Phys. **10**, 859 (2009)
10. G. Garberoglio, A.H. Harvey, J. Res. Natl. Inst. Stand. Technol. **114**, 249 (2009)
11. D. Gugan, G.W. Michel, Metrologia **16**, 149 (1980)
12. C. Gaiser, Doctoral Thesis, Shaker Verlag Aachen. ISBN 978-3-8322-7552-5 (2008)
13. W. Cencek, K. Szalewicz, B. Jeziorski, Phys. Rev. Lett. **86**, 5675 (2001)
14. G. Lach, B. Jeziorski, K. Szalewicz, Phys. Rev. Lett. **92**, 233001 (2004)
15. E. Beth, G.E. Uhlenbeck, Physica **4**, 915 (1937)
16. A. Pais, G.E. Uhlenbeck, Phys. Rev. **116**, 250 (1959)
17. K.H. Berry, Metrologia **15**, 89 (1979)
18. H. Preston-Thomas, Metrologia **27**, 3 (1990)
19. C.P. Chen, S. Mehta, E.A. Hoefling, S. Zelakiewicz, F.M. Gasparini, J. Low Temp. Phys. **102**, 31 (1996)
20. K.A. Rizzo, C. Hättig, B. Fernández, H. Koch, J. Chem. Phys. **117**, 2609 (2002)